International Journal of Pharmaceutics 434 (2012) 199–208

Contents lists available at SciVerse ScienceDirect

International Journal of Pharmaceutics

journal homepage: www.elsevier.com/locate/ijpharm

# Calcium phosphate-mediated gene delivery using simulated body fluid (SBF)

Alireza Nouri[a,*], Rita Castro[a], José L. Santos[a,1], César Fernandes[a,b], João Rodrigues[a], Helena Tomás[a,**]

[a] CQM – Centro de Química da Madeira, MMRG, Universidade da Madeira, Campus Universitário da Penteada, 9000-390 Funchal, Portugal
[b] Laboratório Regional de Engenharia Civil, IP-RAM, Rua Agostinho Pereira de Oliveira, 9000-264 Funchal, Portugal

ARTICLE INFO

*Article history:*
Received 5 April 2012
Received in revised form 18 May 2012
Accepted 21 May 2012
Available online 1 June 2012

*Keywords:*
Simulated body fluid (SBF)
Calcium phosphate
Gene delivery
Transfection

ABSTRACT

The present study aimed at developing a new approach in gene delivery of calcium phosphate nanoparticles through simulated body fluid (CaP-SBF). The physicochemical and biological characteristics of the CaP-SBF nanoparticles were compared with those made in pure water (CaP-water) *via* a similar procedure. The CaP-SBF and CaP-water solutions were then adjusted to two different pH values of 7.4 and 8.0, mixed with plasmid DNA (pDNA), and added in varying amounts to human embryonic kidney (HEK 293T) cells. The transfection efficiency and cell viability were studied *in vitro* by reporter gene (luciferase and Enhanced Green Fluorescent Protein) expression and the resazurin reduction assay, respectively, 24 and 48 h after the incubation with the nanoparticles. Our results indicated considerably high *in vitro* transfection efficiency for CaP-SBF/DNA complexes at physiological pH (7.4) with high amounts of CaP. Additionally, the SBF solution exhibited the ability to reduce the rapid growth of CaP particles over time, leading to higher transfection efficiency of CaP-SBF/DNA complexes than those made in water (CaP-water/DNA).



## 1. Introduction

Gene therapy is becoming a rapidly growing therapeutic strategy for the treatment of both acquired and inherited diseases. The development of safe and efficient gene delivery vectors remains an essential prerequisite for gene therapy. Viral vectors are highly efficient but have significant drawbacks, including high immunogenicity, limited DNA carrying capacity, recombination and high costs. As an alternative system to viral vectors, non-viral vectors have become increasingly attractive for gene therapy due to their low or no immunogenicity, relatively simple preparation procedures, low cost and high flexibility to accommodate the size of the delivered transgene (Santos et al., 2011).

Amongst various non-viral delivery systems, calcium phosphate (CaP) particles offer one of the most attractive methods for gene therapy, and have widely been used as an *in vitro* gene delivery vector for over three decades. The CaP method was first described as a technique to assay the infectivity of DNA from several viruses, as an alternative to the DEAE–dextran method (Graham and Van Der Eb, 1973), however, it became more popular after extending its application to plasmid DNA (pDNA) and gene delivery. The suitability of this method lies in its general efficiency for a wide range of cell lines, simplicity, low cost, as well as biocompatibility, and biodegradability of CaP particles (Jordan, 2000). Different procedures have been used for the synthesis of CaP/DNA complexes including, co-precipitation (Seelos, 1997), encapsulation (Bisht et al., 2005), multi-shell structures formation (Sokolova et al., 2006), and coating of CaP nanoparticles with pDNA (Welzel et al., 2004). According to the current state of knowledge, the CaP/DNA complex precipitates are incorporated into the cells through endocytosis by forming an intracellular vesicle. The vesicles merge with lysosomes and the CaP/DNA particles are released into the cytoplasm. The entrapped DNA somehow escapes from the lysosomes into cytoplasm; and the DNA molecules eventually enter the nuclei of the recipient cells to effect gene transfer and expression (Orrantia and Chang, 1990).

Simulated body fluid (SBF) was first introduced by Kokubo et al. (1990) to analyze the changes in surface-structure of a bioactive glass ceramic. Since then, the SBF solution has routinely been used as an effective *in vitro* testing method to study CaP (apatite) formation or precipitation on the surfaces of different types of biomaterials, in order to predict their *in vivo* bone bioactivity (Chen et al., 2008b; Kokubo and Takadama, 2007; Nouri et al., 2007). The development of SBF is based on the concept that the essential prerequisite to evaluate the bone-binding abilities of a biomaterial is the formation of bone-like apatite layer on its surface when implanted into the living body. Upon the formation of apatite nuclei on a material, they can grow spontaneously by consuming the CaP ions from the surrounding SBF. The inorganic ion concentration

* Corresponding author. Tel.: +351 291705150; fax: +351 291705249.
** Corresponding author.
*E-mail addresses:* nouri@uma.pt (A. Nouri), lenat@uma.pt (H. Tomás).
[1] Present address: Department of Materials Science and Engineering, Johns Hopkins University, 3400 North Charles Street, Baltimore, MD 21218, United States.

0378-5173/$ – see front matter © 2012 Elsevier B.V. All rights reserved.
http://dx.doi.org/10.1016/j.ijpharm.2012.05.066

of the SBF is nearly equal to those of human blood plasma and can reproduce the spontaneous nucleation and growth of bone-like apatite on a variety of biomaterials *in vitro*.

Despite the extensive use of the SBF for testing the bioactivity of hard tissue implants, the chemical synthesis of CaP nanoparticles in SBF solutions instead of pure water has never been explored for gene delivery applications. In the current study, CaP particles were synthesized by precipitation of calcium and phosphate ions in SBF. The physicochemical and biological characteristics of the resultant particles were compared with those made in pure water *via* a similar procedure. The CaP particles synthesized in the SBF solution and water (denoted as CaP-SBF and CaP-water, respectively) were then adjusted to two different pH values (7.4 or 8.0), mixed with pDNA and added in varying amounts to human embryonic kidney 293T (HEK 293T) cell line. The pH (7.4) was chosen due to its physiological relevance and pH (8.0) was selected to study the effect of slight deviation from physiological pH on cell transfection. Finally, the effects of SBF solution, pH, and concentration of CaP particles on gene transfection were investigated.

## 2. Materials and methods

### 2.1. Preparation of SBF

For preparation of the SBF, the following reagents were used: NaCl (Panreac, 99.5%), $NaHCO_3$ (Panreac, 99.7%), KCl (Panreac, 99.5%), $Na_2HPO_4{\cdot}2H_2O$ (Riedel-de Haën, 98.5%), $MgCl_2{\cdot}6H_2O$ (Riedel-de Haën, 99.0%), $CaCl_2$ (Acros, 95.0%), $Na_2SO_4$ (JMGS, 99.5%), Tris [$(CH_2OH)_3CNH_2$] (Merck, 99.8%), and HCl (Riedel-de Haën, 37 vol%).

The preparation and ionic concentration of the SBF solution in the present study are mostly similar to those of reported by Tas (2000), and Kokubo and Takadama (2006). The order, amounts, and concentrations of reagents for preparing 50 mL of SBF are given in Table 1.

### 2.2. Amplification of plasmid DNA

A plasmid DNA (pDNA) encoding for Enhanced Green Fluorescent Protein and luciferase (pEGFPLuc, 6.4 kb) with a cytomegalovirus promoter (CMV) was used. The plasmids were amplified in *Escherichia coli* host strain, DH5α, grown overnight in Luria–Broth Base medium containing antibiotic. Subsequently, the plasmids were isolated and purified by GenElute™ Endotoxin-Free Plasmid maxiprep kit (Sigma–Aldrich). The concentration of pDNA was determined using a Cintra 40 UV–visible Spectrometer (GBC Scientific Equipment) by measuring absorbance at 260/280 nm. The pDNA was suspended in pure water and stored at −20 °C until used.

**Table 1**
Order, amounts, and concentrations of reagents for preparing 50 mL of SBF.

| Order | Reagent | Amount (g) | Concentration (mM) |
|---|---|---|---|
| 1 | NaCl | 0.327 | 112.00 |
| 2 | $NaHCO_3$ | 0.113 | 27.00 |
| 3 | KCl | 0.018 | 5.00 |
| 4 | $Na_2HPO_4{\cdot}2H_2O$ | 0.009 | 1.00 |
| 5 | $MgCl_2{\cdot}6H_2O$ | 0.015 | 1.50 |
| 6 | 1.0 M HCl | ≤0.15 mL | – |
| 7 | $CaCl_2$ | 0.013 | 2.50 |
| 8 | $Na_2SO_4$ | 0.003 | 0.50 |
| 9 | Tris | 0.303 | 50.00 |
| 10 | 1.0 M HCl | ≤2.50 mL | – |

### 2.3. Cell culture

The experiments described here were performed *in vitro* on HEK 293T cells. The cells were incubated in Dulbecco's Modified Eagle's Medium (DMEM, Gibco-BRL), supplemented with 10% fetal bovine serum (FBS), and 1% Antibiotic and Antimycotic solution (AbAm) (all purchased from Gibco) at 37 °C in a humidified atmosphere containing 5% $CO_2$.

### 2.4. Synthesis of CaP and CaP/DNA complexes

CaP nanoparticles were synthesized in two different environments, namely SBF and pure water (Milli-Q, Millipore), which were respectively denoted as CaP-SBF and CaP-water throughout this study. The CaP-water nanoparticles were synthesized to provide us with a better understanding of the effect of SBF solution on the final CaP nanoparticles.

Unlike the traditional CaP transfection procedure in which CaP usually co-precipitates in the presence of pDNA molecules, in the current method the CaP vectors were firstly prepared in the absence of pDNA, and then loaded/mixed with pDNA. Initially, $Ca(NO_3)_2{\cdot}4H_2O$ (Carlo Erba, 99%) and $K_2HPO_4{\cdot}3H_2O$ (Merck, 99%) were used as the calcium and phosphate precursors, respectively. A process flowchart for the preparation of the CaP particles and CaP-DNA complexes is given in Fig. 1. The required amounts of the starting reagents, *i.e.* $Ca(NO_3)_2{\cdot}4H_2O$ and $K_2HPO_4{\cdot}3H_2O$, were added in the SBF solution or pure water in 25 mL glass beakers and dissolved at 700 rpm stirring speed for 5 min. Subsequently, 2.1 mL of the calcium and ~2.6 mL of the phosphate precursors were simultaneously added together in a glass beaker and stirred at 700 rpm stirring speed for 5 min. The calcium and phosphate ions in the precursor solutions spontaneously react to form the CaP

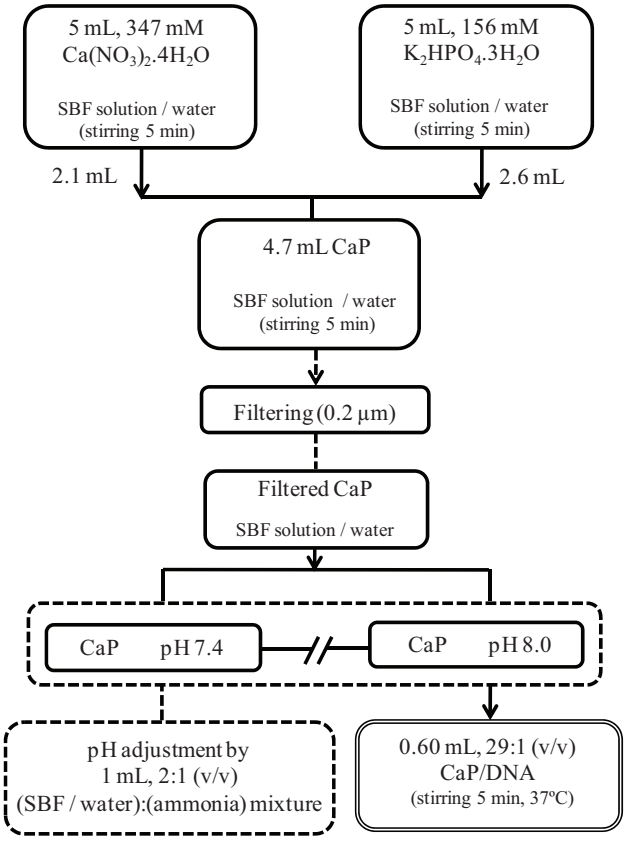


**Fig. 1.** Process flowchart for synthesis of CaP-SBF/DNA and CaP-water/DNA complexes.

precipitates upon mixing together. No pH adjustment was carried out before and during the synthesis. The final pH values of the CaP-SBF and CaP-water solutions after the synthesis and before the filtering process were, respectively, 7.1 and 5.8. The resultant CaP-SBF or CaP-water solutions were filtered through a 0.2 μm cellulose acetate filter (VWR International). The pH of the filtered solutions was adjusted to 7.4 and 8.0 using 2:1 (v/v) of the SBF or water with $NH_4OH$ solution (Riedel-de Haën, 33 vol%). 580 μL of each CaP-SBF and CaP-water solutions, in either pH of 7.4 or 8.0, were separately added to 20 μL of pDNA solution (containing 20 μg of pDNA), placed in a 37 °C water bath, and stirred at 700 rpm stirring speed for 5 min. The appropriate amounts of CaP-SBF/DNA and CaP-water/DNA complexes (*i.e.* 25, 50, and 100 μL) were then immediately added to the appointed wells containing 500 μL of the DMEM culture medium, supplemented with 10% FBS and 1% AbAm.

### 2.5. Characterization of CaP nanoparticles

The X-ray diffraction patterns of the CaP-SBF and CaP-water nanoparticles were recorded using a powder X-ray diffractometer (D8 Advance, Bruker AG). Prior to the filtering process, the CaP particles were collected and centrifuged 3 times (8850 × *g*, 5 min, RT). The CaP powders were thoroughly washed with pure water between each centrifugation process and dried by a conventional lyophilization technique. The diffractometer used Cu Kα radiation (λ = 1.5418 Å) and was operated at 30 kV and 40 mA. All samples were run for 1 h in the 2$\theta$ range 5–100°.

Fourier transform infrared spectroscopy (FTIR) of the CaP particles was assessed using attenuated total reflectance (ATR) technique by a Vertex 70, Bruker. Specac Golden Gate™ was used as an ATR accessory. During the test, the samples were purged with dry, $CO_2$-free nitrogen. All of the spectra were collected in the 4000–400 $cm^{-1}$ wavenumber range.

In order to find the difference in final mass between the CaP particles made in the SBF solution and water, an experiment was devised. Firstly, 9.4 mL of either CaP-SBF or CaP-water solutions was synthesized by adding 4.2 mL of calcium and 5.2 mL of phosphate precursors in their respective environments. The resultant aqueous suspensions of particles were transferred into centrifuge tubes (30 mL) and were subjected to centrifugation for 10 min at 10,000 × *g* and at room temperature. The deposit was washed twice by re-suspension in pure water and centrifuged, and finally dried at 37 °C. The obtained dried mass of the CaP-SBF and CaP-water solutions was 0.131 and 0.086 g, respectively. This considerable difference between the masses suggests the denser aqueous suspensions of particles in the CaP-SBF solution, and it can be due to the fact that the SBF solution already contained calcium and phosphate ions. A slight turbidity was observed upon the addition of calcium and phosphate precursors into the SBF solution as a result of an immediate reaction between the pre-existing calcium and phosphate ions in the SBF solution with their counterparts in the precursors.

### 2.6. PicoGreen intercalation assay

The interaction between pDNA and the CaP nanoparticles was determined using the PicoGreen® (Invitrogen) assay. The fluorescence intensity of PicoGreen increases significantly upon binding with free pDNA. Complexes between pDNA and varying concentrations (0–10.15 μL) of CaP-SBF and CaP-water at two different pH values of 7.4 and 8.0 were prepared in pure water using 0.2 μg of pDNA in a final volume of 100 μL. Meanwhile, PicoGreen reagent was 200-fold diluted in TE buffer (10 mM Tris, 1 mM EDTA, pH 7.5) and 100 μL of the solution was added to each complex. The resultant mixtures were allowed to stand for 5 min at room temperature and protected from the light. The mixtures were added to an opaque 96-well plate and PicoGreen fluorescent emission was measured in the microplate reader (model Victor$^3$ 1420, PerkinElmer) at $\lambda_{ex}$ = 485 nm, $\lambda_{em}$ = 535 nm.

The measurements were carried out in triplicates and the relative fluorescence percentage (%*F*) was determined using the following equation:

$$\%F = \frac{F_{\text{complex}} - F_{\text{blank}}}{F_{\text{free DNA}} - F_{\text{blank}}} \times 100$$

It is notable that the fluorescence from free DNA is considered 100%.

### 2.7. Particle size analysis and Zeta potential measurement

Dynamic light scattering (DLS) with a Zetasizer Nano-ZS (Malvern) was used to measure the particle size and zeta potential of the CaP-SBF/DNA and CaP-water/DNA complexes. Keeping the same ratio of CaP solution to pDNA (29:1), a total volume of 800 μL of complexes was prepared as described earlier. The particle size of the freshly prepared complexes was measured at 25 °C with a scattering angle of 173°, and the zeta potential was determined by the standard capillary electrophoresis cell of Zetasizer Nano ZS with a detection angle of 17° at 25 °C. All the average values were performed with the data from three separate measurements. The growth of CaP nanoparticles, in the presence and absence of DMEM culture medium, was also monitored by measuring the change in size at different time intervals including 1, 3, 6, and 24 h.

### 2.8. Optical density (OD) measurements

The OD measurement was carried out to quantify the rate of CaP particle growth by measuring the turbidity of the CaP solutions in the presence or absence of DMEM at varying incubation time periods of 1, 3, 6, and 24 h. For this reason, two well plates (24 wells each) were chosen and in each well 200 μL of either CaP-SBF or CaP-water solutions were added to 1 mL of DMEM. Prior to addition of CaP solutions, the pH of DMEM was adjusted to 7.4 to resemble the real conditions of the test. The samples in 24 well plates were incubated at 37 °C in a humidified atmosphere containing 5% $CO_2$ and their absorbance was measured at different time intervals of 1, 3, 6, and 24 h using UV spectrometer at 320 nm. Meanwhile, the growth of CaP-SBF and CaP-water nanoparticles at room temperature and without using DMEM was monitored by measuring their OD at similar time intervals.

### 2.9. Cytotoxicity tests

The cytotoxicity of CaP-SBF/DNA and CaP-water/DNA complexes was determined 24 h post-transfection using the HEK 293T cell line. Cytotoxicity was evaluated by determining the percentage of cell viability using the resazurin reduction assay that establishes a correlation between the cellular metabolic activity and the number of viable cells in culture (Page et al., 1993). 50 μL of resazurin reagent was added to the each well and the plate was incubated for 3 h in a humidified atmosphere with 5% $CO_2$ at 37 °C. Subsequently, the resultant medium was transferred to 96-well opaque plates (Nunc) using 100 μL/well and the resorufin fluorescence ($\lambda_{ex}$ = 530 nm, $\lambda_{em}$ = 590 nm) was measured in the microplate reader. Untreated cells were taken as control with 100% viability. All experiments were run in triplicate from two independent measurements.

### 2.10. In vitro transfection procedure and luciferase activity measurement

A day before transfection, HEK 293T cells were seeded at density of $6 \times 10^4$ cells/well onto 24-well tissue culture plates (Corning) along with 1 mL of DMEM medium containing serum and antibiotics. Cells were transfected at approximately 60% confluence. One hour before transfection, the cell culture medium in each well was replaced with 500 μL fresh serum-containing medium. Subsequently, the transfection was performed by adding the CaP-SBF/DNA (or CaP-water/DNA) complexes in varying amounts of 25, 50 and 100 μL to each well. The complexes were allowed to remain in the cell culture medium overnight, after which the cell culture medium was replaced with 1 mL serum-containing medium.

Forty-eight hours post transfection, the medium was removed and 100 μL Reporter Lysis Buffer 1× (RLB) was added to each well and the plates were stored at −80 °C overnight. Cell lysates were analyzed for luciferase activity with Promega's luciferase assay reagent. The relative light units (RLU) were normalized against protein concentration in the cell extracts. The protein concentration was determined using the bicinchoninic acid assay (BCA assay) with bovine serum albumin as a standard. The transfection efficiency was characterized by firefly luciferase expression and denoted as relative light units per mg of protein (RLU $mg^{-1}$ protein) ± standard deviation. All samples were carried out in triplicate and two independent experiments were performed to verify the reproducibility.

### 2.11. Fluorescence microscopy

EGFP expression studies were carried out 48 h after transfection, using a fluorescent inverted microscope (TE2000-E, Nikon). The NIS Elements Advanced Research software was used to acquire pictures of the transfected cells.

### 2.12. Statistics

All statistical analyses were performed using IBM SPSS Statistics 19 software (IBM Inc., Armonk). Results are reported as mean ± standard deviation. One-way ANOVA with Tukey *Post Hoc* test were used to assess the statistical differences between the group means.

## 3. Results

### 3.1. Characterization of CaP nanoparticles

The X-ray diffraction patterns (Fig. 2) revealed a high degree of crystallinity for CaP-SBF and CaP-water, as represented by sharp diffraction peaks of the materials. From the angle of the obtained peaks, we have evaluated that the major peaks are characteristic of the dicalcium phosphate dihydrate structure (DCPD; $CaHPO_4{\cdot}2H_2O$), commonly known as brushite. No significant difference was found in the XRD patterns between CaP-SBF and CaP-water particles. However, the CaP-SBF patterns revealed small peaks of NaCl, due to the high concentration of NaCl (112 mM) in the SBF solution.

FTIR analyses were performed to further characterize the chemical structure of CaP-SBF and CaP-water nanoparticles, as shown in Fig. 3. Similar to the XRD patterns, no remarkable difference was found between the FTIR spectra of CaP nanoparticles prepared in the SBF solution and water. The FTIR spectra of the CaP nanoparticles showed intense and broad bands assigned to O—H stretching and bending of $H_2O$ (1645 and 3435 $cm^{-1}$), and two bands corresponding to $CO_3^{2-}$ groups ($\upsilon_3$ mode at 1645 $cm^{-1}$ and $\upsilon_2$ mode at 874 $cm^{-1}$), indicating the presence of $CaCO_3{\cdot}PO_4^{3-}$ groups were located at 1216–984 $cm^{-1}$ ($\upsilon_3$ mode), and at 874 $cm^{-1}$ ($\upsilon_1$ mode). The absorption band located at around 870 $cm^{-1}$ is a common band in all spectra which can be due to either $HPO_4$ group or due to $\upsilon_2$ band of $CO_3^{2-}$. FTIR spectra verified previous XRD analyses that phosphate and hydrogen phosphate bands are characteristic of brushite structure (1220, 1130, 1055, and 986 $cm^{-1}$ for P—O $\upsilon_3$ mode, 874 $cm^{-1}$ for P—O(H) $\upsilon_1$ mode and 520 $cm^{-1}$ for P—O $\upsilon_4$ mode) (Barrere et al., 2002).

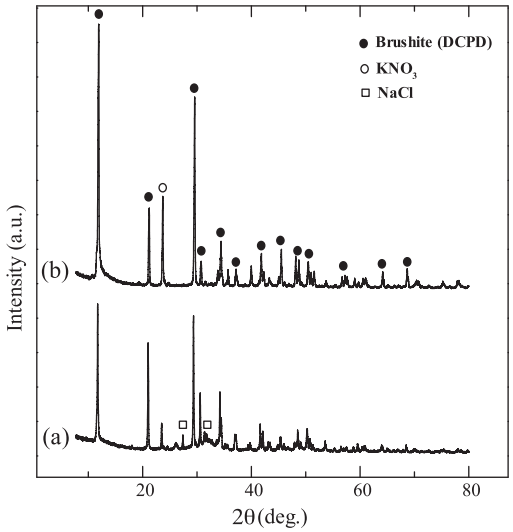


**Fig. 2.** XRD spectra of CaP particles synthesized in (a) SBF solution (CaP-SBF); and (b) pure water (CaP-water).

### 3.2. Characterization of CaP/DNA complexes

The extent of pDNA condensation with CaP particles was evaluated by performing the PicoGreen test. As shown in Fig. 4, the fluorescence intensity decreased with increasing amount of CaP/DNA, suggesting more tightly condensed complexes at larger amount of CaP. The CaP-water at pH (7.4) appeared to be the most tightly bound to pDNA than other tested samples, as indicated by higher percent reduction in fluorescence intensity. However,

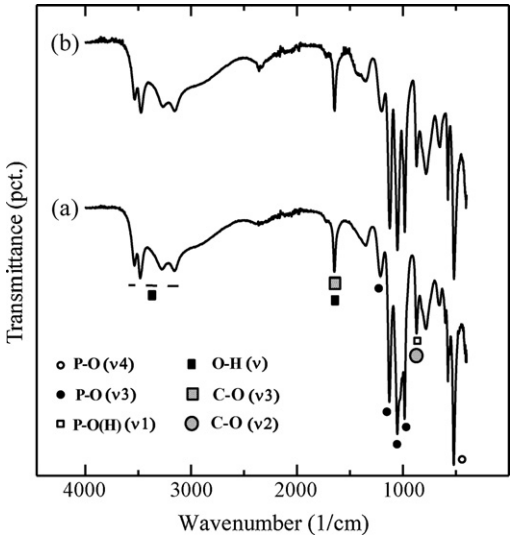


**Fig. 3.** FTIR spectra of CaP particles synthesized in (a) SBF solution (CaP-SBF); and (b) pure water (CaP-water).

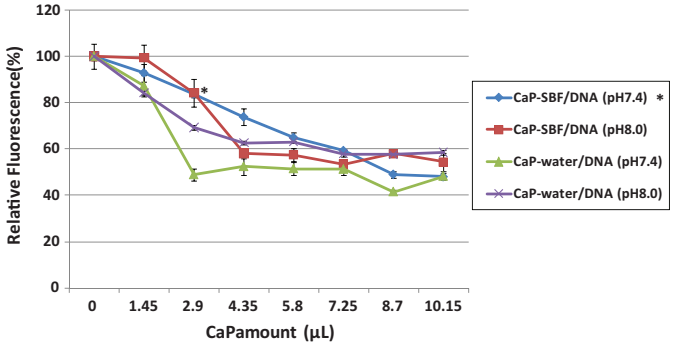


**Fig. 4.** The percentage of bound pDNA with CaP nanoparticles was quantified by PicoGreen (PG) assay. The results are reported as the relative percentage of PG fluorescence, where 100% intensity was observed for a CaP-free solution (only pDNA). $^{*}p < 0.05$ when the CaP-SBF/DNA complexes are compared to CaP-water/DNA at the same CaP amount and pH value.

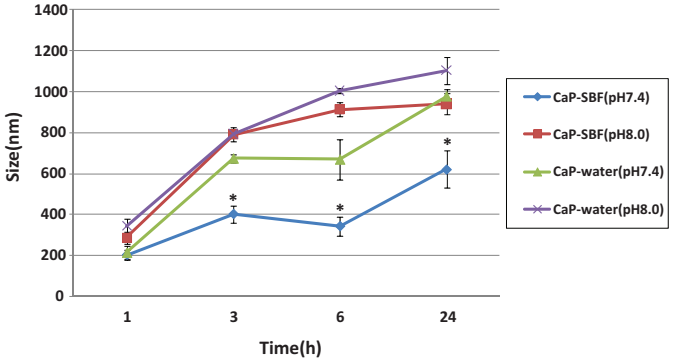


**Fig. 5.** Determination of particle growth by measuring the CaP particle diameter at pH values of 7.4 and 8.0. The CaP-SBF and CaP-water solutions were incubated in DMEM culture medium at 37 °C and 5% $CO_2$ and the particle size was assessed at different incubation times of 1, 3, 6 and 24 h. $^{*}p < 0.05$ when the CaP-SBF particles are compared to CaP-water particles at the same time period and pH value.

at CaP amount of ≥4.35 μL, the CaP-SBF (pH 8.0) showed slightly better pDNA binding ability than CaP-water at the same pH value.

### 3.3. Particle size analysis and zeta potential

In the present study, the size of CaP particles was measured immediately after synthesis to avoid any aggregation or particle growth that might occur over time. Table 2 summarizes the particle size and zeta potential of CaP-SBF and CaP-water particles and complexes at two different pH values. As listed in Table 2, CaP-SBF (pH 7.4) particles exhibited smaller size than CaP-water particles at the same pH value, with the average particle diameter (*z*-average) of 105 nm and 220 nm, respectively. The size of CaP particles increased upon mixing with pDNA, yet a smaller size was obtained for those made in the SBF solution. A similar trend was also observed with increasing pH value of the CaP solutions to 8.0, indicating smaller particle size for CaP-SBF and CaP-SBF/DNA compared to their counterparts made in water. However, increasing pH (8.0) resulted in larger CaP particles than those formed at pH (7.4).

The average zeta potential for the CaP-SBF particles and CaP-SBF/DNA complexes was more negative (or less positive) than CaP-water particles and CaP-water/DNA complexes for both pH values. No considerable difference in zeta potential was observed between pH values in a given CaP solution. CaP particles without pDNA carry almost no charge or slightly positive charge. Complexation with pDNA renders the particles strongly negative, with the average of −18 and −14 mV for CaP-SBF/DNA and CaP-water/DNA, respectively.

**Table 2**
Particle size and zeta potential of CaP-SBF and CaP-water particles and their complexes with pDNA at two pH values of 7.4 and 8.0.

| Sample | Particle size (nm) | Zeta potential (mV) |
|---|---|---|
| CaP-SBF (pH 7.4) | 104.9 ± 19.8* | −0.8 ± 1.6 |
| CaP-SBF (pH 8.0) | 348.6 ± 28.8 | 0.3 ± 1.8 |
| CaP-water (pH 7.4) | 219.9 ± 21.5 | 2.8 ± 1.1 |
| CaP-water (pH 8.0) | 384.3 ± 32.2 | 2.9 ± 1.4 |
| CaP-SBF/DNA (pH 7.4) | 323.1 ± 34.8 | −18.9 ± 1.3 |
| CaP-SBF/DNA (pH 8.0) | 444.9 ± 55.0 | −18.8 ± 2.0* |
| CaP-water/DNA (pH 7.4) | 390.2 ± 32.4 | −14.7 ± 0.9 |
| CaP-water/DNA (pH 8.0) | 461.4 ± 56.6 | −14.1 ± 1.5 |

The data is presented as average size ± standard error ($n = 3$).
* In a statistical analysis, $p < 0.05$ when CaP-SBF particles and complexes are compared to CaP-water particles and complexes, respectively, and at the same pH value.

### 3.4. CaP particle growth

DLS measurements also indicated a growth in particle size over time for all CaP samples. Fig. 5 demonstrates the particle size as a function of time for CaP-SBF and CaP-water particles at pH values of 7.4 and 8.0. The CaP particles were immersed in DMEM and incubated at 37 °C and 5% $CO_2$; and the growth in particle size was evaluated 1, 3, 6, and 24 h after incubation. As shown in Fig. 5, the most rapid growth occurred between 1 and 3 h in all tested samples. The CaP particles grew larger when prepared in water, as indicated by steeper and larger size of CaP-water particles than those made in the SBF at varying time intervals. This difference in particle growth is particularly more noticeable at pH 7.4 between CaP-SBF and CaP-water. Increasing the pH value to 8.0, enhanced the growth rate of CaP particles for both the SBF- and water-made samples. However, after 24 h, the CaP-SBF (pH 7.4) particles showed the lowest growth rate with the mean particle diameter of 620 nm. The CaP-water particles experienced the most dramatic growth rates over the entire period.

The growth in particle size and density of CaP particles can also be determined by measuring the OD of CaP solutions as addressed by Jordan (2000) and Jordan and Wurm (2004). The OD, also referred as turbidity test, was quantified by measuring the absorbance at 320 nm with a UV spectrophotometer. Normally, higher OD values are typical for mixtures with an increasing particle size or/and an increasing number of particles, which render the solution visibly opaque. Fig. 6 represents the OD values (320 nm) of the CaP particles incubated in the presence and absence of DMEM at different time periods of 1, 3, 6, and 24 h. In the presence of DMEM (as illustrated in columns) and at pH value of 7.4, the OD values of the CaP-water solution were considerably higher than CaP-SBF solution, indicating the higher turbidity (*i.e.* particle size) of the former. However, a somewhat similar trend was observed between the CaP-SBF and CaP-water solutions at higher pH value of 8.0. Increasing the pH also resulted in higher OD values. The OD values (320 nm) of CaP particles at different time periods were also measured at ambient temperature and without using the DMEM culture medium. The results have been represented in Fig. 6 with straight lines and markers. The CaP-water (pH 7.4) showed averagely 23% increase in its OD values as compared to that of CaP-SBF (pH 7.4). It can also be seen that the turbidity of the CaP-water at pH of 7.4 was even higher than CaP-SBF at pH of 8.0. Likewise, the CaP-water (pH 8.0) presented the highest absorbance among the samples. An increase in absorption at 320 nm indicates the growth of precipitates (or higher density), which could be confirmed

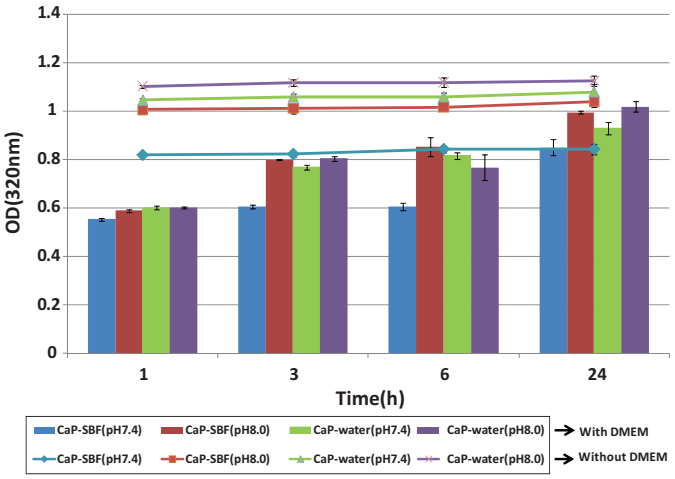


**Fig. 6.** Optical density (OD) was used as an indicator of CaP particle growth or precipitation by measuring the turbidity of CaP particles at 320 nm. The OD results were determined from an aqueous suspension of CaP incubated in the presence and absence of DMEM culture medium and at 37 °C and 5% $CO_2$; at ambient temperature.

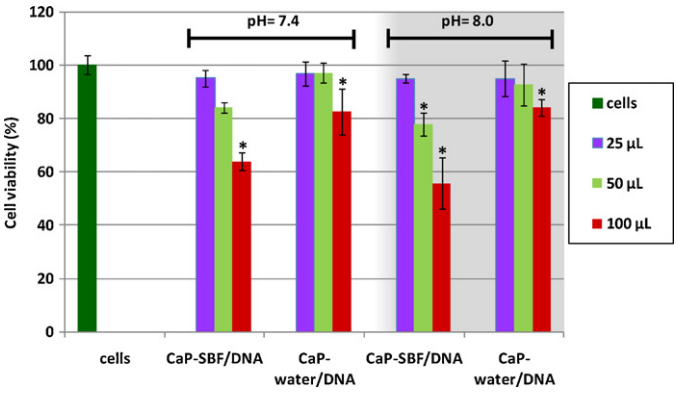


**Fig. 8.** The cell viability of HEK 293T cells, 24 h post-transfection with CaP-SBF/DNA and CaP-water/DNA complexes. The complexes were obtained at two pH values (7.4 and 8.0) for varying amounts of CaP complexes in cell culture medium. $^*p < 0.05$ when the complexes are compared with cells.

visually. These findings are in agreement with the results obtained from size measurement at different time periods (see Fig. 5).

Fig. 7 shows microscopic images of the CaP particles formed 24 h after incubation in DMEM culture medium at 37 °C and 5% $CO_2$. The images were taken from CaP-SBF and CaP-water particles at two varying pH of 7.4 and 8.0. The CaP-SBF (pH 7.4) represented the smallest particles among other samples, distributed evenly on the bottom of the well. However, the CaP-water solution at the same pH showed coarser particles, while some degree of aggregation was also observed. A significant increase in particle size and aggregation was observed when the pH value increased to 8.0 (esp. for the CaP-water particles).

### 3.5. Cytotoxicity of CaP/DNA complexes

The cytotoxicity of CaP/DNA complexes was evaluated in HEK 293T cell line 24 h post-transfection, using the resazurin reduction assay. Untreated cells served as a negative control. At large amount of CaP/DNA complex (*i.e.* 50 and 100 µL), the complexes formed in pure water were less toxic than those made in the SBF solution, as shown in Fig. 8. The reduction in cell viability appeared in a dose-dependent manner, reaching the minimum values at 100 µL (CaP/DNA)/well. In particular, when the HEK 293T cells were treated by CaP-SBF/DNA (pH 8.0), the loss of cell viability attained as high as 45%. However, no significant difference was observed between the cell viability of the CaP complexes at low amount of CaP complex (25 µL), indicated by a minor degree of cell death at this dose.

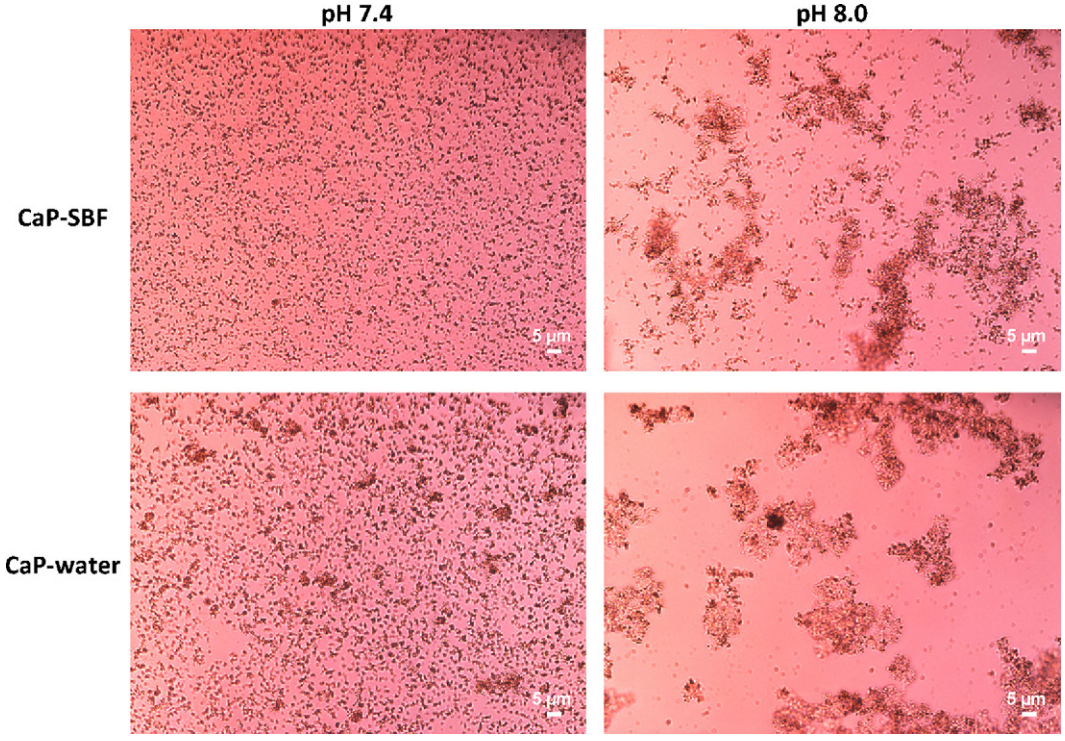


**Fig. 7.** Microscopic images of CaP-SBF and CaP-water precipitates 24 h after incubation in DMEM culture medium at 37 °C and 5% $CO_2$. The experiment was carried out by adding aqueous suspension of CaP-SBF and CaP-water at two different pH values of 7.4 and 8.0.

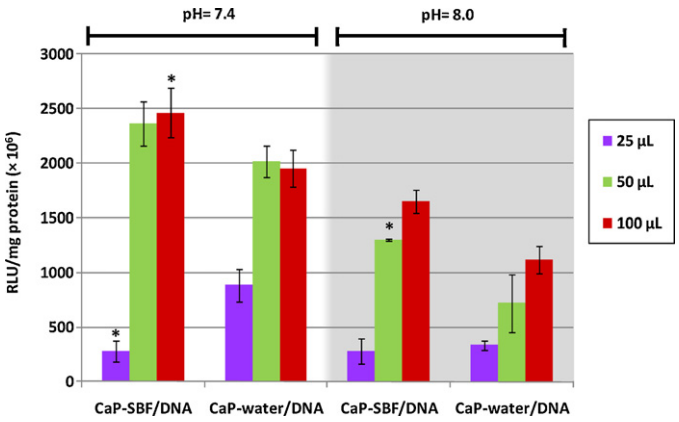


**Fig. 9.** *In vitro* luciferase expression in HEK 293T cells transfected with CaP-SBF/DNA and CaP-water/DNA complexes prepared at two pH values of 7.4 and 8.0. Cells were harvested 48 h after transfection, and luciferase activities were determined. $^{*}p < 0.05$ when the CaP-SBF/DNA complexes are compared to CaP-water/DNA complexes at the same amount and pH value.

### 3.6. In vitro transfection studies

The gene transfection efficiency of the CaP/DNA complexes was assessed *in vitro* using luciferase and GFP reporter genes (pEGFP-Luc) into HEK 293T cells. The CaP/DNA complexes were immediately added to wells, containing 500 μL DMEM (supplemented with serum and antibiotic), at varying amounts (*i.e.* 25, 50 and 100 μL) and incubated overnight. Luciferase activity was determined 48 h-post transfection and normalized against protein content (Fig. 9). The CaP/DNA amounts were chosen based on a series of preliminary experiments to test the effect of CaP amounts on transfection efficiency.

Enhanced transfection efficiency was observed by increasing amount of CaP/DNA complexes, showing the highest transfection efficiency at 100 μL for CaP-SBF (pH 7.4). The CaP-SBF/DNA complexes showed higher transfection efficiency at both pH values of 7.4 and 8.0, as compared to CaP-water/DNA complexes in similar pH values. The difference in transfection efficiency was more pronounced at pH (8.0) between CaP-SBF/DNA and CaP-water/DNA complexes at larger amount of CaP/DNA complex. Nevertheless, higher transfection efficiency was achieved when the CaP/DNA complexes at pH (7.4) were used.

Fig. 10 shows fluorescence micrographs of the CaP/DNA complexes synthesized at two pH values (7.4 and 8.0) and three various CaP/DNA amounts of 25, 50 and 100 μL. The obtained fluorescence images were in agreement with the luciferase reporter assay data. It was noticeable that the number of green fluorescent cells increased with increasing amount of CaP/DNA complexes in wells. It was also observed that at higher amounts of CaP, larger number of cells was transfected with CaP-SBF/DNA complexes than CaP-water/DNA.

## 4. Discussion

### 4.1. Characterization of CaP nanoparticles

The drop in pH values of the SBF solution and water after the synthesis of CaP particles lies in the formation of calcium and phosphate particles upon incorporation of hydroxyl groups (OH) to crystal lattice, which in fact favors the formation of brushite. Brushite is the most predominant CaP phase often formed in more acidic aqueous solutions. Formation of brushite at pH lower than 6.5 has been reported in several studies (Cheng and Pritzker, 1983; Giocondi et al., 2010; Wang and Nancollas, 2008). Theoretically, brushite should form even at physiological pH and temperature, when the product of the concentrations of total calcium and total inorganic phosphate is sufficiently large (Cheng and Pritzker, 1983). Brushite is endowed with an excellent biocompatibility, grows and dissolves readily, and has a comparatively fast nucleation rate due to its low surface energy (Giocondi et al., 2010).

### 4.2. Size and zeta potential

The size and surface charge of particles are considered to be the key factors for successful gene delivery into mammalian cells. Small and positively charged particles are easily taken up by cells and would lead to high gene expression (Chowdhury et al., 2004; Epple et al., 2010). The surface charge of particles is mainly controlled by adsorption of multiply charged ions, the ionic strength of the solution, pH, as well as the particle size and shape (Zhu et al., 2004).

The increase in ionic strength will reduce the Debye length, and will subsequently shield the surface charge and reduce the zeta potential (Morgan, 2010). In an experiment with seawater, Beckett and Le (1990) noted that NaCl on its own cannot account for the reduction in surface charge of the suspended particles and the presence of minor divalent cations such as $Mg^{2+}$ and $Ca^{2+}$ in the solution are more effective in reducing the surface charge of the particles than the major monovalent cations like $Na^{+}$. Thus, the lower zeta potential of the CaP-SBF particles and complexes can be contributed to the higher ionic strength and also multiply charged ions of the SBF solution when compared to pure water.

Calcium-deficient and/or relatively phosphate-rich condition of the CaP particles can also give rise to their net negative surfaces (Zhu et al., 2004). The magnitude of the negative zeta potential increases in response to the decrease in Ca/P ratio. In a theoretical study performed by Bastos et al. (2008), interactions between calcium and two buffer systems, namely Tris and Bis-tris, were investigated in standard and modified SBF solutions. The results revealed that the Tris/Bis-tris-buffered SBF solutions reduce the content of available calcium ion, with a stronger trend towards Bis-tris. They reasoned that with buffer, the complexation reaction $Ca^{2+} + PO_4^{3-} \rightleftharpoons CaPO_4^{-}$ is slightly displaced towards to free phosphate direction, making the phosphate more available. The above results had also been experimentally confirmed by Serro and Saramago (2003). They prepared a SBF solution with the same composition of Kokubo SBF (Kokubo and Takadama, 2006), but without the buffer Tris. It was shown that the Tris-buffered SBF solution formed soluble complexes with several cations, including the most important $Ca^{2+}$. Thus, it is envisaged that the $Ca^{2+}$ ions chelated by Tris in the SBF solution lowers Ca/P molar ratio and consequently, affect the surface charge and binding abilities of the CaP-SBF particles as compared with CaP-water particles. However, one should not expect a large difference in Ca/P molar ratio between the CaP-SBF and CaP-water particles since the XRD analyses of the both particles showed similar diffraction peaks revealing brushite as their major peaks. Brushite has a Ca/P molar ratio of 1, in comparison with the stoichiometric value of 1.6 for hydroxyapatite.

The negatively charged pDNA reversed the initially positive or neutral surface charge of the CaP particles to negative values, as seen by drastically lower zeta potential of the CaP particles after complexation with pDNA (Table 2). On the other hand, a fairly similar trend in surface charge variation of the particles with pH is indicating that the surface charges of the CaP particles after the synthesis were not affected by the adsorption of $H^{+}$ and $OH^{-}$ ions. It is believed that pDNA binding ability is associated with the surface charge of the particles. Thus, it comes as no surprise that the more positively charged CaP-water particles promote higher binding ability to the negatively charged pDNA, as seen in Fig. 4.

### 4.3. Size and particle growth

The variation in size of CaP-SBF and CaP-water particles stems from the difference in rate of CaP crystal growth between

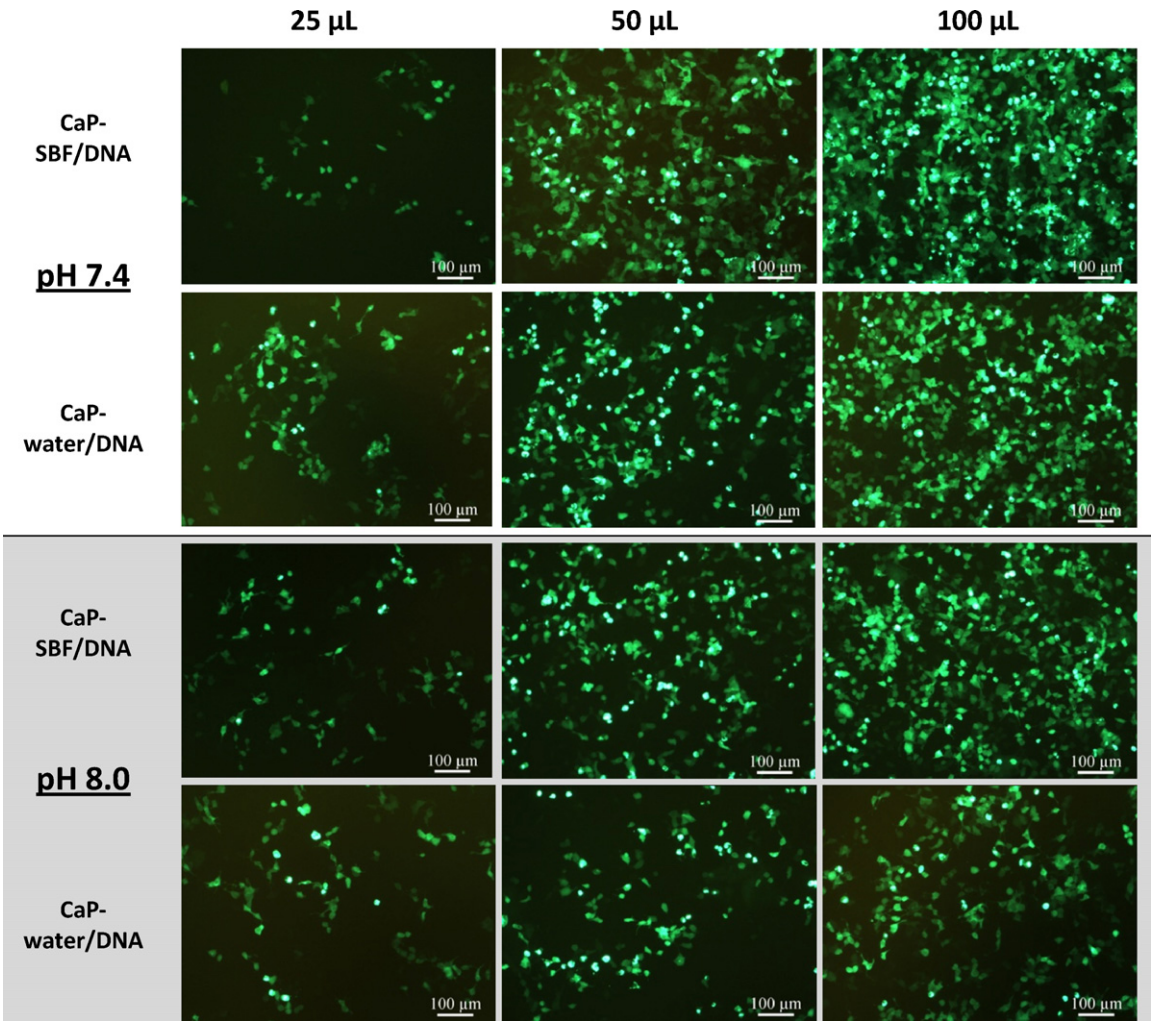


**Fig. 10.** Enhanced Green Fluorescent Protein (EGFP) expression in HEK 293T cells transfected using CaP-SBF/DNA and CaP-water/DNA complexes with pH values of 7.4 and 8.0. The CaP/DNA complexes were added in varying amounts of 25, 50 and 100 µL to cell culture wells containing 500 µL of DMEM (supplemented with 10% FBS and 1% AbAm). The fluorescence microscopy images were taken 48 h post-transfection.

SBF- and water-mediated solutions. This uncontrollable rapid growth of CaP crystals is one of the major limitations of the CaP method, resulting in poor reproducibility and the formation of large aggregates (>µm) to considerably reduce the transfection efficiency. Conditions which affect the solubility of CaP precipitates would directly affect the rate of CaP crystal growth. The solubility of CaP precipitates in a solution/culture medium, is in turn affected by several parameters including ionic strength, the composition of the solution, and the pH value of the solution (Jordan, 2000). Increasing the NaCl content, *i.e.* ionic strength, enhances the solubility of the CaP precipitates and decrease its growth and rapid precipitation, since NaCl simply reduces the driving force for reaction (Nancollas and Tomazic, 1974). Barrere et al. (2002) reported a delay in CaP precipitation on a Ti alloy soaked in a 5 times concentrated SBF solution (SBF × 5), by increasing the ionic strength. It appeared that increasing NaCl content lowers the nucleation sites in the solution and thereby decrease the CaP precipitation.

The composition of a solution also affects the solubility of CaP precipitates. For instance, increasing the calcium concentration decreases solubility, and lead to rapid precipitation of CaP crystals, especially at basic pH values (Jordan, 2000). As previously pointed out, Tris forms soluble complexes with $Ca^{2+}$ and reduces the concentration of free $Ca^{2+}$ ions in SBF. It can also inhibit growth through physical adsorption on the surface of CaP crystals (Kanzaki et al., 1998). In addition, the pH value of the Tris-buffered solution remains at a stable, relatively low value (7.4 ± 0.1), hindering CaP precipitation (Marques et al., 2003). In general, biological fluids contain ions and molecules that interfere with CaP precipitation *in vitro*. Molecules and ions are usually adsorbed on the surface of CaP precipitates and, thus, reducing the formation and/or growth of CaP critical nuclei and crystals (Blumenthal, 1989). As reported by Lu and Leng (2005), the higher concentration of $HCO_3^-$ (27 mM) in SBF than pure water can also reduce the driving force for precipitation. It is also very well known that the solubility of CaP in a solution increases with a decrease of pH (Elliot, 1994). Similarly, the lack of ionic strength and interfering ions in water-mediated solutions resulted in the rapid growth and aggregation of particles over time (as seen in Fig. 7 for CaP-water particles). However, both the CaP-SBF and CaP-water particles grew in size with increasing incubation time due to further consumption of the calcium and phosphate ions from the solution.

### 4.4. Cytotoxicity of CaP/DNA complexes

Although the CaP method is classified as a relatively safe gene delivery system (since this is in the GRAS list of FDA) (Roy et al., 2003), the CaP nanoparticles can adversely affect cell viability. In the CaP method, the inhibiting cell proliferation and cell damage typically continue in a dose- and time-dependent manner and increase with higher amount of CaP nanoparticles

and longer incubation time (Motskin et al., 2009). Larger amount of CaP nanoparticles can produce too much $Ca^{2+}$ for the cell to survive. Cells need to maintain a very low intracellular $Ca^{2+}$ concentration, and an overload in cellular $Ca^{2+}$ has been suggested to be the pathway of cell death (Yu et al., 2001).

The chemical composition of the transfection medium plays an important role in cell survival. The lower cell viability of the CaP-SBF/DNA than CaP-water/DNA complexes can be attributed to the presence of multiple ions and molecules in the SBF solution. In a study on the effect of ions in dispersion of rat liver cells, Seglen (1973) reported the maximum stimulations by higher concentrations of divalent cations such as $Ca^{2+}$ and $Mg^{2+}$, while $K^+$, $SO_4^{2-}$ and $HPO_4^{2-}$ appeared to have less or no effect in inhibiting enzymatic dispersion. The buffer Tris, present in SBF, is also known to be inhibitory in certain biological systems due to the availability of primary amine and hydroxyl groups on Tris molecule for reactivity (Fernandez et al., 1993).

Although the precise pH value for optimal cell growth varies with the individual cell lines, any significant deviation from the physiological pH range (*i.e.* 7.2–7.6) may lead to impediment of cell growth/proliferation and alter the metabolic rate (Ceccarini and Eagle, 1971), as seen by lower degree of cell viability at higher pH (8.0) than pH (7.4) for both complexes and in particular for CaP-SBF/DNA. As a result, the CaP-SBF/DNA complex at amounts of 25 and 50 μL/well at two different pHs lie in an acceptable level of cell viability.

### 4.5. In vitro transfection studies

Despite the lower DNA-binding ability and lower zeta potential of CaP-SBF particles than CaP-water particles, *in vitro* transfection studies on HEK 293T cells revealed higher gene expression for the former. This is surprising since a decrease in zeta potential represents a reduction in the electrostatic interaction between the CaP particles and the pDNA. On the other hand, the lower the DNA-binding ability (lower extent of DNA condensation), the less effectively is the DNA bound to the CaP nanoparticles, which also results in low transfection efficiency. Therefore one might expect a different response *in vitro*. Such discrepancy could be mainly attributed to the smaller particle size and lower degree of particle growth in CaP-SBF particle as compared to CaP-water particles. In another words, the resulting lower transfection efficiency in CaP-water/DNA complexes is indicating that most of the CaP-water/DNA complexes were too large to enter the cells. Rapid growth of the CaP-water particles resulted in sharp increase in diameter which is a big hurdle for efficient gene delivery and expression into the cells.

However, due to the more CaP nuclei per unit volume in the SBF-CaP than CaP-water solution, it would be rational to expect that covering cells with numerous small CaP/DNA complexes instead of a few larger ones increase the chances of pDNA to be transfected into the nucleus.

The uncontrollable rapid growth of CaP particles always leads to bulk and highly aggregated precipitates, which induces low transfection efficiencies (Wang et al., 2010). The results from DLS and OD at different incubation time periods revealed more physical stability for CaP-SBF solution at pH (7.4), reducing the rapid formation of coarse precipitates. Thus, the CaP-SBF/DNA complex is gradually formed in the culture medium during incubation and precipitates on the cells. Physical stability is an important advantage for *in vivo* applications, as nanoparticles do not have to be used immediately after preparation. In a high pH environment, the CaP/DNA mixture will form coarse precipitates that aggregate into large clumps in the medium and significantly reduce the transfection efficiency (Chen et al., 2008a).

The valuable aspect of SBF solution in gene delivery applications was its impact in reducing rapid particle growth and aggregation in solution and culture medium. The resulting formation of relatively small and stable CaP-SBF particles/complexes at longer incubation time gave rise to high transfection efficiency in HEK 293T cell line at physiological pH.

## 5. Conclusions

In an attempt to investigate the application of simulated body fluid (SBF) in gene delivery, calcium and phosphate (CaP) nanoparticles were synthesized in a SBF solution and mixed with pDNA. The *in vitro* gene transfection studies revealed that the pEGFP-Luc plasmid could effectively be transfected by the CaP-SBF/DNA complex at physiological pH (7.4). The results were also compared with those using CaP particles made in pure water (CaP-water) *via* a similar procedure. Despite the lower DNA-binding ability and lower zeta potential of CaP-SBF particles in comparison with CaP-water particles, the *in vitro* studies showed higher transfection efficiency for CaP-SBF/DNA complexes than for CaP-water/DNA. The SBF solution showed the ability to reduce the rapid growth of CaP particles over time, leading to smaller particles as compared to those synthesized in pure water. These findings provide new insights into the role of SBF solution in synthesis of CaP particles for gene delivery applications.

## Acknowledgments

The Fundação para a Ciência e a Tecnologia (FCT, Portugal) is acknowledged for funding through the project PEst-OE/QUI/UI0674/2011 (CQM, Portuguese Government funds). The support of FCT through the Post-Doc grant awarded to A. Nouri (SFRH/BPD/47369/2008) is also acknowledged. Additionally, authors are grateful to Dr. T. Segura (UCLA, USA) and to INEB (Porto, Portugal) for kindly providing the EGFPLuc-pDNA and the cell line, respectively. The authors also wish to thank the support of UMa, through the Santander bank Chair in Nanotechnology, and LREC (Laboratório Regional de Engenharia Civil–Madeira).

## References

Barrere, F., van Blitterswijk, C.A., de Groot, K., Layrolle, P., 2002. Influence of ionic strength and carbonate on the Ca–P coating formation from SBF × 5 solution. Biomaterials 23, 1921–1930.

Bastos, I.N., Platt, G.M., Andrade, M.C., Soares, G.D., 2008. Theoretical study of Tris and Bistris effects on simulated body fluids. J. Mol. Liq. 139, 121–130.

Beckett, R., Le, N.P., 1990. The role or organic matter and ionic composition in determining the surface charge of suspended particles in natural waters. Colloids Surf. 44, 35–49.

Bisht, S., Bhakta, G., Mitra, S., Maitra, A., 2005. pDNA loaded calcium phosphate nanoparticles: highly efficient non-viral vector for gene delivery. Int. J. Pharm. 288, 157–168.

Blumenthal, N.C., 1989. Mechanisms of inhibition of calcification. Clin. Orthop. Relat. Res. 247, 279–289.

Ceccarini, C., Eagle, H., 1971. pH as a determinant of cellular growth and contact inhibition. Proc. Natl. Acad. Sci. U.S.A. 68, 229–233.

Chen, C.Y.A., Ezzeddine, N., Shyu, A.B., 2008a. Messenger RNA half-life measurements in mammalian cells. Methods Enzym. 448, 335–357.

Chen, X.B., Nouri, A., Li, Y.C., Lin, J.G., Hodgson, P.D., Wen, C.E., 2008b. Effect of surface roughness of Ti, Zr, and TiZr on apatite precipitation from simulated body fluid. Biotechnol. Bioeng. 101, 378–387.

Cheng, P.T., Pritzker, K.P.H., 1983. Solution Ca/P ratio affects calcium phosphate crystal phases. Calcif. Tissue Int. 35, 596–601.

Chowdhury, E.H., Kunou, M., Nagaoka, M., Kundu, A.K., Hoshiba, T., Akaike, T., 2004. High-efficiency gene delivery for expression in mammalian cells by nanoprecipitates of Ca–Mg phosphate. Gene 341, 77–82.

Elliot, J.C., 1994. Structure and Chemistry of the Apatites and Other Calcium Orthophosphates. Elsevier, Amsterdam, The Netherlands.

Epple, M., Ganesan, K., Heumann, R., Klesing, J., Kovtun, A., Neumann, S., Sokolova, V., 2010. Application of calcium phosphate nanoparticles in biomedicine. J. Mater. Chem. 20, 18–23.

Fernandez, R.D., Yoshimizu, M., Ezura, Y., Kimura, T., 1993. Comparative growth response of fish cell lines in different media, temperatures, and sodium chloride concentrations. Fish Pathol. 28, 27–34.
Giocondi, J.L., El-Dasher, B.S., Nancollas, G.H., Orme, C.A., 2010. Molecular mechanisms of crystallization impacting calcium phosphate cements. Philos. Trans. R. Soc. A 368, 1937–1961.
Graham, F.L., Van Der Eb, A.J., 1973. A new technique for the assay of infectivity of human adenovirus 5 DNA. Virology 52, 456–467.
Jordan, M., 2000. Transient gene expression in mammalian cells based on the calcium phosphate transfection method. In: Al-Rubeai, M. (Ed.), Cell Engineering: Transient Expression. Kluwer Academic Publishers, pp. 56–79.
Jordan, M., Wurm, F.M., 2004. Transfection of adherent and suspended cells by calcium phosphate. Methods 33, 136–143.
Kanzaki, N., Onuma, K., Ito, A., Teraoka, K., Tateishi, T., Tsutsumi, S., 1998. Direct growth rate measurement of hydroxyapatite single crystal by moire phase shift interferometry. J. Phys. Chem. B 102, 6471–6476.
Kokubo, T., Kushitani, H., Sakka, S., Kitsugi, T., Yamamuro, T., 1990. Solutions able to reproduce in vivo surface-structure changes in bioactive glass–ceramic A–W. J. Biomed. Mater. Res. 24, 721–734.
Kokubo, T., Takadama, H., 2006. How useful is SBF in predicting in vivo bone bioactivity? Biomaterials 27, 2907–2915.
Kokubo, T., Takadama, H., 2007. Simulated body fluid (SBF) as a standard tool to test the bioactivity of implants. In: Epple, M., Baeuerlein, E. (Eds.), Handbook of Biomineralization: Medical and Clinical Aspects. Wiley-VCH, Weinheim, pp. 97–108.
Lu, X., Leng, Y., 2005. Theoretical analysis of calcium phosphate precipitation in simulated body fluid. Biomaterials 26, 1097–1108.
Marques, P.A.A.P., Serro, A.P., Saramago, B.J., Fernandes, A.C., Magalhães, M.C.F., Correia, R.N., 2003. Mineralisation of two calcium phosphate ceramics in biological model fluids. J. Mater. Chem. 13, 1484–1490.
Morgan, T.T., 2010. Thesis: Synthesis and characterization of bioresorbable calcium phosphosilicate nanocomposite particles for fluorescence imaging and biomedical applications. Department of Chemistry, The Pennsylvania State University.
Motskin, M., Wright, D.M., Muller, K., Kyle, N., Gard, T.G., Porter, A.E., Skepper, J.N., 2009. Hydroxyapatite nano and microparticles: correlation of particle properties with cytotoxicity and biostability. Biomaterials 30, 3307–3317.
Nancollas, H., Tomazic, B., 1974. Growth of calcium phosphate on hydroxyapatite crystals. Effect of supersaturation and ionic medium. J. Phys. Chem. 78, 2218–2225.
Nouri, A., Chen, X.B., Hodgson, P.D., Long, J.M., Yamada, Y., Wen, C.E., 2007. Preparation of bioactive porous Ti–Sn–Nb alloy for biomedical applications. In: 5th International Conference on Porous Metals and Metallic Foams (MetFoam), pp. 307–310.
Orrantia, E., Chang, P.L., 1990. Intracellular distribution of DNA internalized through calcium phosphate precipitation. Exp. Cell Res. 190, 170–174.
Page, B., Page, M., Noel, C., 1993. A new fluorometric assay for cytotoxicity measurements in vitro. Int. J. Oncol. 3, 473–476.
Roy, I., Mitra, S., Maitra, A., Mozumdar, S., 2003. Calcium phosphate nanoparticles as novel non-viral vectors for targeted gene delivery. Int. J. Pharm. 250, 25–33.
Santos, J.L., Pandita, D., Rodrigues, J., Pêgo, A.P., Granja, P.L., Tomás, H., 2011. Non-viral gene delivery to mesenchymal stem cells: methods, strategies and application in bone tissue engineering and regeneration. Curr. Gene Ther. 11, 46–57.
Seelos, C., 1997. A critical parameter determining the aging of DNA–calcium-phosphate precipitates. Anal. Biochem. 245, 109–111.
Seglen, P.O., 1973. Preparation of rat liver cells. II. Effects of ions and chelators on tissue dispersion. Exp. Cell Res. 76, 25–30.
Serro, A.P., Saramago, B., 2003. Influence of sterilization on the mineralization of titanium implants induced byincubation in various biological model fluids. Biomaterials 24, 4749–4760.
Sokolova, V.V., Radtke, I., Heumann, R., Epple, M., 2006. Effective transfection of cells with multi-shell calcium phosphate-DNA nanoparticles. Biomaterials 27, 3147–3153.
Tas, A.C., 2000. Synthesis of biomimetic Ca-hydroxyapatite powders at 37 °C in synthetic body fluids. Biomaterials 21, 1429–1438.
Wang, K.W., Zhou, L.Z., Sun, Y., Wu, G.J., Gu, H.C., Duan, Y.R., Chen, F., Zhu, Y.J., 2010. Calcium phosphate/PLGA-mPEG hybrid porous nanospheres: a promising vector with ultrahigh gene loading and transfection efficiency. J. Mater. Chem. 20, 1161–1166.
Wang, L., Nancollas, G.H., 2008. Calcium orthophosphates: crystallization and dissolution. Chem. Rev. 108, 4628–4669.
Welzel, T., Radtke, I., Meyer-Zaika, W., Heumann, R., Epple, M., 2004. Transfection of cells with custom-made calcium phosphate nanoparticles coated with DNA. J. Mater. Chem. 14, 2213–2217.
Yu, S.P., Canzoniero, L.M.T., Choi, D.W., 2001. Ion homeostasis and apoptosis. Curr. Opin. Cell Biol. 13, 405–411.
Zhu, P., Masuda, Y., Koumoto, K., 2004. The effect of surface charge on hydroxyapatite nucleation. Biomaterials 25, 3915–3921.